Spectroscopic, Electrochemical, and Photochemical Studies of Self-Assembled via Axial Coordination Zinc Porphyrin−Fulleropyrrolidine Dyads†

Francis D'Souza,*,‡ Gollapalli R. Deviprasad,‡ Melvin E. Zandler,‡ Vu T. Hoang,‡ Arkady Klykov,‡ Michael VanStipdonk,‡ Asiri Perera,‡ Mohamed E. El-Khouly,§ Mamoru Fujitsuka,§ and Osamu Ito*,§

Department of Chemistry, Wichita State University, 1845 Fairmount, Wichita, Kansas 67260-0051, and Institute of Multidisciplinary Research for Advanced Materials, Tohoku University, Katahira, Sendai, 980-8577, Japan

Received: August 20, 2001; In Final Form: January 24, 2002

Spectroscopic, redox, and photochemical behavior of self-assembled donor−acceptor dyads formed by axial coordination of zinc tetraphenylporphyrin, (TPP)Zn, and fulleropyrrolidine bearing either pyridine or imidazole coordinating ligands were investigated. The UV−vis, ^{1}H NMR, and ESI-mass spectral studies, as well as computational studies, revealed supramolecular 1:1 dyad formation between the electron donor [(TPP)Zn] and the electron acceptor, fulleropyrrolidine entities. The determined formation constant *K* values followed the order *o*-pyridyl ≪ *m*-pyridyl ≃ *p*-pyridyl ≪ *N*-phenyl imidazole entities of the fulleropyrrolidine. The evaluated thermodynamic parameters revealed stable complexation with complex dissociation enthalpies ranging between 26 and 32 kJ mol^{-1}. The ^{1}H NMR studies revealed axial coordination of the pyridine or imidazole ligands to the central zinc of (TPP)Zn, while the ESI-Mass spectral studies performed in CH_2Cl_2 matrix revealed the expected molecular ion peak of the self-assembled dyads. The geometric and electronic structures of the dyads were probed using ab initio B3LYP/3-21G(*) methods. Such studies revealed stable complexation between (TPP)Zn and fulleropyrrolidine entities. The majority of the highest occupied frontier molecular orbital (HOMO) was found to be located on the (TPP)Zn entity, while the lowest unoccupied molecular orbital (LUMO) was found to be entirely on the fullerene entity. The redox behavior of the isolated self-assembled dyads was investigated in *o*-dichlorobenzene, 0.1 (TBA)ClO_4. A total of seven one-electron redox processes corresponding to the oxidation and reduction of zinc porphyrin ring, and the reduction of fullerene entities were observed within the accessible potential window of the solvent. These electrochemical results suggest weak interactions between the constituents in the ground state. The excited-state electron-transfer reactions were monitored by both steady-state and time-resolved emission as well as transient absorption techniques. In *o*-dichlorobenzene, upon coordination of either the pyridine or imidazole entities of fulleropyrrolidine to (TPP)Zn, the main quenching pathway involved charge separation from the singlet excited (TPP)Zn to the C_{60} moiety. The calculated rate of charge separation was found to range between 10^7 and 10^{10} s^{-1} depending upon the axial ligand (pyridine or imidazole) of the fulleropyrrolidine. However, in a coordinating solvent like benzonitrile, intermolecular electron transfer predominantly takes place mainly from the triplet excited (TPP)Zn to the C_{60} moiety. The present studies also revealed little or no quenching of the singlet excited fulleropyrrolidine upon coordination of (TPP)Zn.

Introduction

Studies on donor−acceptor dyads capable of undergoing light-induced electron- or energy transfer are of current interest to mimic the primary events of the photosynthetic reaction center and also to develop molecular electronic devices.[1,2] Toward constructing such dyads, fullerenes[3] are particularly appealing as electron acceptors[4] because of their three-dimensional structure,[5] low reduction potentials,[6] and absorption spectra extending over most of the visible region.[7] Accordingly, a number of covalently linked photosensitizer constituent-fullerene complexes have been investigated.[8−11] Such donor−acceptor complexes undergo photoinduced electron and/or energy transfer upon excitation of the constituents.

Among the different routes to form dyads, self-assembled donor−acceptor conjugates are particularly appealing since they are more biomimetic to the natural photoenergy conversion systems.[2a−d] Recently, a self-assembly method involving zinc tetrapyrrole and C_{60} via axial ligation of the central metal ion has been described.[11] For this, zinc tetrapyrroles were used as electron donors while pyridine appended fullerene derivatives were used as electron acceptors. Efficient quenching of the donor emission was observed upon coordinating the pyridine functionalized fullerenes. To gain further insights into the axial coordination governed self-assembly process, and to evaluate the factors responsible for the stability, we have performed a systematic study by using different substituted fulleropyrrolidines. That is, we have employed 2-(*o*-, *m*-, or *p*-pyridyl)-fulleropyrrolidine, **1**−**3**, *N*-methyl-2-(*p*-pyridyl)fulleropyrrolidine, **4**, as well as 2-(4′-imidazolylphenyl)fulleropyrrolidine, **5**, as acceptors (Scheme 1). The pyrrolidine nitrogen in compounds

† Presented in part at the 199th meeting of the Electrochemical Society, Washington, D.C., March 2001, paper no. 738.

‡ Wichita State University.

§ Tohoku University.

10.1021/jp013165i CCC: $22.00
Published on Web 03/08/2002

SCHEME 1

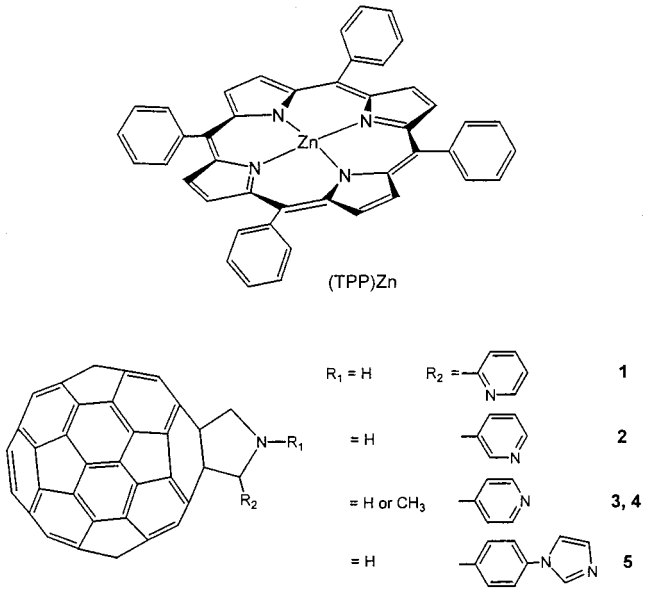

1−**3** and **5** is a secondary amine, while in **4** it is a tertiary amine, with each type of nitrogen having a relatively low basicity compared to that of pyrrolidine.[12] The imidazole bearing fulleropyrrolidine, developed in the present study, is expected to result in more stable self-assembled dyads due to its higher basicity. The molecular stoichiometry, association constants, and thermodynamic parameters have been evaluated by using optical absorption methods. Elucidation of the molecular geometry has been performed using ^{1}H NMR and mass spectral studies. Computational studies using ab initio B3LYP/3-21G(*) methods have been performed to elucidate the geometry and electronic structure of the dyads, and the results have been compared with the recently reported crystal structure of (TPP)Zn:**4** dyad.[11d]

The different photochemical events (electron transfer) originating from the excited singlet and triplet states of zinc porphyrin as well as from the excited singlet and triplet states of fulleropyrrolidine (Scheme 2) have been probed by using different photochemical techniques. Using steady-state emission method, the effect of the bound fullerene on the singlet emission of (TPP)Zn and singlet emission of fulleropyrrolidine have been monitored. Both picosecond time-resolved and nanosecond transient absorption spectral studies have been systematically performed in order (i) to evaluate the rates of light induced electron-transfer reactions, (ii) to characterize the electron-transfer products, and (iii) to differentiate between the intramolecular versus intermolecular electron-transfer reactions in the self-assembled donor−acceptor dyads.

Experimental Section

Chemicals. Buckminsterfullerene, C_{60} (+99.95%) was from BuckyUSA (Bellaire, TX). *o*-Dichlorobenzene and benzonitrile in sure seal bottles, glycine, sarcosine, *o*-, *m*-, and *p*-pyridine carboxaldehyde, and 4-imidozolyl benzaldehyde were from Aldrich Chemicals (Milwaukee, WI). All chemicals were used as received. Syntheses and purification of (TPP)Zn were carried out according to the literature procedure.[13]

Fulleropyrrolidine derivatives bearing pyridine or imidazole ligands, **1**−**5**, was prepared according to a general procedure of fulleropyrrolidine synthesis developed by Prato and coworkers.[14] For this, a mixture of C_{60} (100 mg), glycine (31 mg) or sarcosine (31 mg), and (*o*-, *m*- or *p*-)pyridine carboxaldehyde (68 μL) or 4-imidazolyl benzaldehyde (52 mg) in toluene (60 mL) was refluxed for 4−12 h. At the end, the solvent was removed under reduced pressure. The crude product was dissolved in toluene and purified over a silica gel column using 1:1 ethyl acetate and toluene as eluent (yield = 20−45%). The compounds were recrystallized from CS_2 and methanol (1:1 v/v) solvent mixture. **(1)** ^{1}H NMR in CS_2:$CDCl_3$ (1:1 v/v), δ: 5.71, 5.10, 4.84 (s, d, d, *J*7, *J*7, 3H, pyrrolidine-H), 8.73, 7.77, 7.27 (d, q, m, *J*8, *J*7, *J*7, 4H, pyridine-H). λ_{max} in *o*-dichlorobenzene, 309.4 and 433.1 nm. **(2)** FAB mass in CH_2Cl_2, cald 840.8, found 841.1. δ: 5.80, 5.13, 4.88 (s, d, d, *J*7, *J*7, 3H, pyrrolidine-H), 8.59, 7.38, 8.19, 9.05 (d, q, d, *J*7, *J*6, *J*7, s, 4H, pyridine-H). λ_{max} in *o*-dichlorobenzene, 310.0 and 430.2 nm. **(3)** δ: 5.73, 5.09, 4.86 (s, d, d, *J*7, *J*7, 3H, pyrrolidine-H), 8.62, 7.69 (d, d, *J*7, *J*7, 4H, pyridine-H). λ_{max} in *o*-dichlorobenzene, 311.3 and 429.2 nm. **(4)** δ: 4.99, 4.92, 4.28 (d, s, d, *J*6, *J*7, 3H, pyrrolidine-H), 8.65, 7.70 (d, d, *J*7, *J*8, 4H, pyridine-H), 2.81 (s, 3H, *N*-methyl-H). λ_{max} in *o*-dichlorobenzene, 308.5 and 431.0 nm. **(5)** ^{1}H NMR in CS_2:$CDCl_3$ (1:1 v/v), δ ppm, 4.90, 5.10, 5,83 (d,d,s, *J*7, *J*7, 3H, pyrrolidine-H), 7.96, 7.45 (d,d, *J*6, *J*6, 4H, phenyl-H), 7.57, 7.99 (d,d, *J*7, *J*7., 2H, imidazol-H), 7.82 (s, 1H, imidazol-H). FAB mass in CH_2Cl_2, cald 905.1, found 905.2. λ_{max} in *o*-dichlorobenzene, 310.2 and 428.1 nm.

SCHEME 2

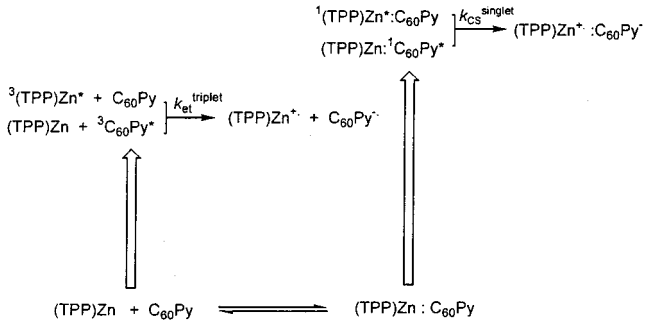

Instrumentation. The UV−vis spectral measurements were carried out with a Shimadzu Model 1600 UV-vis spectrophotometer. The fluorescence emission was monitored by using a Spex Fluorolog-tau spectrometer. A right angle detection method was used. The ^{1}H NMR studies were carried out either on a Varian 400 MHz or Varian 300 MHz spectrometers. Tetramethylsilane (TMS) was used as an internal standard. All the solutions were purged prior to spectral measurements using argon gas. The computational calculations were performed by semiempirical PM3 and ab initio B3LYP/3-21G(*) methods with GAUSSIAN 98[15] software package on various PCs and a SGI ORIGIN 2000 computer. The graphics of HOMO and LUMO coefficients were generated with the help of *GaussView* software. The ESI-Mass spectral analyses of the self-assembled complexes were performed by using a Fennigan LCQ-Deca mass spectrometer. The starting compounds and the dyads (about 1 mM concentration) were prepared in CH_2Cl_2, freshly distilled over calcium hydride

Time-Resolved Emission and Transient Absorption Measurements. Nanosecond transient absorption spectra in the NIR region were measured by means of laser-flash photolysis; 532 nm light from a Nd:YAG laser was used as the exciting source and a Ge-avalanche-photodiode module was used for detecting the monitoring light from a pulsed Xe-lamp as described in our previous report.[16] The picosecond time-resolved fluorescence spectra were measured using an argon-ion pumped Ti:sapphire laser (Tsunami) and a streak scope (Hamamatsu Photonics). The details of the experimental setup are described elsewhere.[16]

Results and Discussion

Formation and Characterization of Self-Assembled via Axial Coordination (TPP)Zn:C_{60} Dyads. Figure 1 shows the

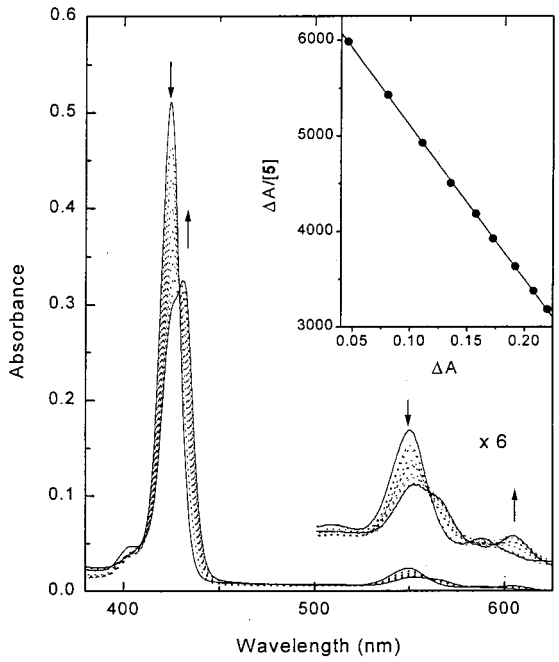

Figure 1. UV−vis spectral changes observed during the complexation of (TPP)Zn (2 μM) and **5** in *o*-dichlorobenzene. The inset figure shows the Scatchard plot of the change of absorbance at 421 nm.

UV−vis optical absorption spectral changes observed during the complexation of **5** with (TPP)Zn. The formation of penta-coordinated zinc porphyrin complex was characterized by diminished Soret band intensity, red-shifted visible bands, and appearance of isosbestic points at 429, 559, 580, and 595 nm.[17] However, for compound **1**, that is, the *ortho*-pyridine-substituted fulleropyrrolidine, little or no spectral changes were observed indicating negligible amount of axial coordination. Job's plot of continuous variation method also confirmed 1:1 complex formation between the (TPP)Zn and compounds **2**−**5** in solution. To confirm that the pyridine or the imidazole unit of compounds **2**−**5** was involved in coordination and not the pyrrolidine nitrogen, control experiments involving 2-phenyl fulleropyrrolidine, i.e., a compound bearing phenyl ring instead of pyridine, was also performed.[11a] No spectral changes were observed during the titration of 2-phenyl fulleropyrrolidine with (TPP)Zn indicating the absence of axial coordination through the pyrrolidine nitrogen.

In agreement with the UV−vis spectral results, the ^{1}H NMR studies performed in $CDCl_3$:CS_2 (1:1 v/v) revealed binding of pyridine or imidazole group of fulleropyrrolidine to the metal ion of (TPP)Zn. Figure 2 shows the ^{1}H NMR spectral data for **5** in the absence and presence of (TPP)Zn. The β-pyrrole and phenyl ring protons of (TPP)Zn in the 7−9 ppm region experienced a shielding of nearly 0.2 ppm upon coordinating **5**. Interestingly, this shielding was found to be more for the imidazole protons of compound **5** in the 6−7.5 ppm region owing to the influence of porphyrin ring current effects.[13] That is, the imidazole protons of **5** experienced up to 2 ppm shielding while this effect for the phenyl ring proton (7−8 ppm) adjacent to imidazole and pyrrolidine ring protons (4.5−6.0 ppm) was about 1 ppm. These results were consistent with the axial coordination of the imidazole entity to the zinc metal center.

The formation constant K for (TPP)Zn:C_{60} dyads were obtained from the absorption spectral data by using Scatchard method (Figure 1 inset).[18] Table 1 lists the K values along with the thermodynamic parameters evaluated from van't Hoff plots of ln K vs T^{-1}. The binding and thermodynamic parameters for

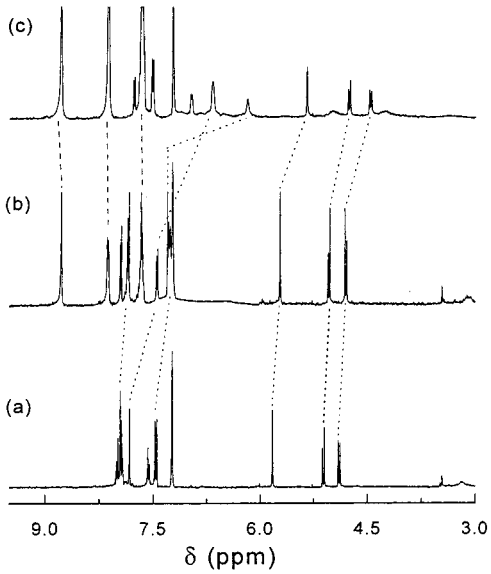

Figure 2. ^{1}H NMR spectrum of (a) **5** (10 mM), (b) **5** (10 mM) and (TPP)Zn (0.5 mM), and (c) **5** (10 mM) and (TPP)Zn (10 mM) in $CDCl_3$:CS_2 (1:1 v/v).

TABLE 1: Formation Constant *K* and the Thermodynamic Parameters for Self-assembled Zinc Tetraphenylporphyrin−Fulleropyrrolidine Conjugates in *o*-Dichlorobenzene

ligand	K,[a] M^{-1}	ΔG, kJ mol^{-1}	ΔH, kJ mol^{-1}	ΔS, JK^{-1}mol^{-1}
pyridine[b]	7 749	−22.1	−27.3	−17.1
N-phenyl imidazole	18 615	−24.0	−32.4	−28.2
1	*c*			
2[b]	7 737	−22.1	−26.1	−12.3
3	7 659	−22.1	−26.7	−15.4
4	7 169	−22.0	−26.9	−16.5
5	11 609	−23.6	−31.9	−28.1

[a] At 298 K. [b] From ref 11a. [c] No appreciable binding was observed.

pyridine and N-phenyl imidazole binding to (TPP)Zn are also listed in Table 1 for comparison purposes. An examination of Table 1 reveals the following: The K values are 5−10% smaller for fulleropyrrolidine appended pyridine or phenyl imidazole compared with the ones bearing no C_{60} entity. The trend in K values follows: *o*-pyridyl ≪ *m*-pyridyl ≃ *p*-pyridyl ≪ *N*-phenyl imidazole substituted fulleropyrrolidines. The observed higher value for **5** compared to **2**−**4** is consistent with the higher basicity of imidazole ring. The evaluated thermodynamic parameters ($-\Delta G$, $-\Delta H$, and $-\Delta S$) also follow a similar trend (Table 1). That is, both entropy and enthalpy changes contribute to the overall free-energy change. Between **3** and **4**, that is, fulleropyrrolidine with secondary and tertiary pyrrolidine nitrogen, the K value is nearly 8% lower for **4**, due to the interaction between CH_3 and phenyl ring in (TPP)Zn (this can be presumed from Figure 4).

The relatively high values of K obtained for the self-assembled dyads in the present study further prompted us to characterize them by using mass spectroscopic technique. Figure 3 shows the electron spray ionization mass spectrum of pristine (TPP)Zn, **5**, and the self-assembled dyad, (TPP)Zn:**5**. The positive ion mass spectrum of (TPP)Zn in CH_2Cl_2 revealed the m/z peak at 676 along with a weaker band at m/z = 709 corresponding to the methanol coordinated species, which is probably formed during recrystallization. The negative ion mass spectrum of **5** revealed a peak at m/z at 905 corresponding to its molecular ion peak. The negative ion mass spectrum of the (TPP)Zn:**5** obtained by either slow precipitation of (TPP)Zn and

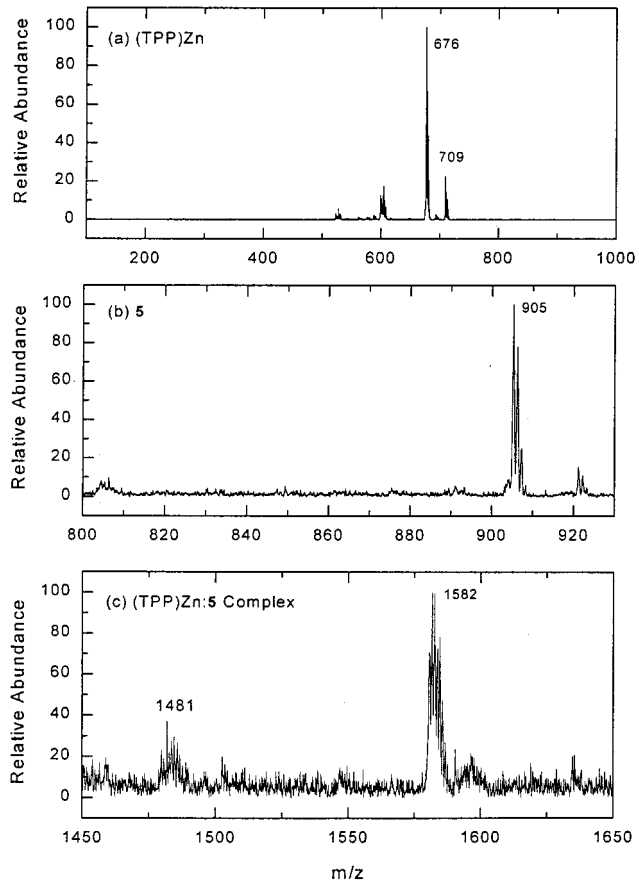

Figure 3. Electron spray ionization mass spectrum of (a) (TPP)Zn, (b) **5**, and (c) (TPP)Zn:**5** complex in CH_2Cl_2 matrix.

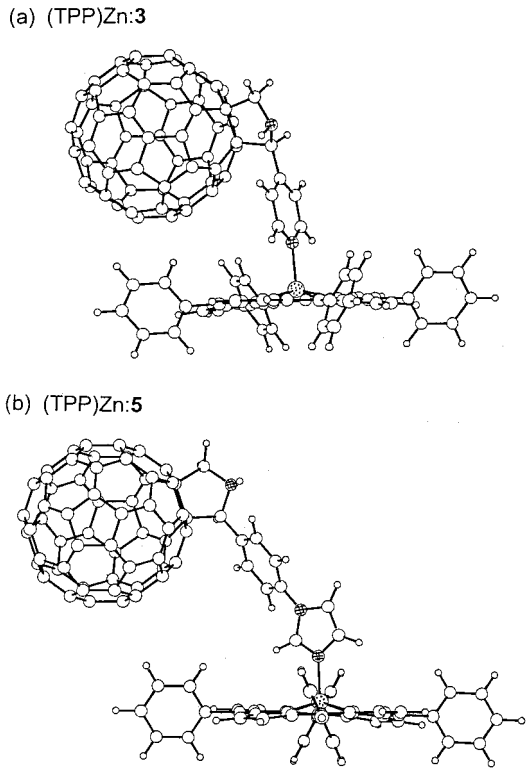

Figure 4. Ab initio B3LYP/3-21G(*) energy optimized structure of (a) (TPP)Zn:**3** and (b) (TPP)Zn:**5** supramolecular dyads. Hatched circle: nitrogen. Dotted circle: zinc.

5 in CH_2Cl_2/*n*-hexane or mixing equimolar amounts of (TPP)Zn and **5** in CH_2Cl_2 revealed a peak at $m/z = 1582$ corresponding to the molecular ion peak of the self-assembled dyad. Similar results were also obtained for (TPP)Zn:**3** or (TPP)Zn:**4** dyads suggesting the existence of the self-assembled complexes in the gas phase.

Computational Studies. To gain insights into the molecular geometry and electronic structure, computational studies were performed by using ab initio B3LYP/3-21G(*)[15] methods on the zinc porphyrin-fulleropyrrolidine dyads and the geometries were compared to the recently reported X-ray structure of (TPP)Zn:**4** dyad.[11d] For this, first, both the starting compounds, (TPP)Zn and 2-substituted fulleropyrrolidines were fully optimized to a stationary point on the Born−Openheimer potential energy surface and allowed to interact. The geometric parameters of the conjugates were obtained after complete energy minimization. Figure 4 shows the calculated structures for (TPP)Zn:**3** and (TPP)Zn:**5** dyads. The Zn:N distance of the newly formed axial coordination bond was found to be ~ 2.06 Å which was almost similar to the bond distances of four other Zn−N bonds of the zinc porphyrin ring. The center-to-center distance, that is, the distance between the central zinc and the center of the C_{60} spheroid, was found to be ~9.98 Å for the (TPP)Zn:**3** dyad which compared with a distance of 10.4 Å for the (TPP)Zn:**4** dyad at the same computational level, and ~9.53 Å calculated from the X-ray structure of the (TPP)Zn:**4** dyad. However, for the (TPP)Zn:**5** dyad, the center-to-center distance was found to be 12.26 Å, that is, a nearly 2.2 Å larger separation between the donor−acceptor entities as compared to the pyridine bound dyads. The X-ray structure determined edge-to-edge distance between the porphyrin macrocycle (*meso*-carbon) and C_{60} entity was found to be 3.186 Å for the (TPP)Zn:**4** dyad, which compared with the computed distance of 4.69 Å (β-pyrrole) for the same dyad, 4.42 Å for the (TPP)Zn:**3** dyad, and 6.91 Å for the (TPP)Zn:**5** (*meso*-C) dyad. These results suggest a larger donor−acceptor separation for (TPP)Zn:**5** dyad as compared to the other ones.

The B3LYP/3-21G* calculated bond dissociation energy for the newly formed the axial coordinate bond, that is, the energy difference between the dyad and the sum of the energies of (TPP)Zn and fulleropyrrolidine were found to be 121.8, 120.9, and 133.5 kJ mol^{-1}, respectively, for the (TPP)Zn:**3**, (TPP)-Zn:**4** and (TPP):**5** dyads. These values are higher than the experimentally determined heat of dissociation for the axial bond (Table 1) of 26.7, 26.9, and 31.9 kJ mol^{-1} for the same series of dyads, but show the same trend of bond energies. No BSSE corrections were made. Interestingly, the semiempirical PM3 computed values were found to be 24.2, 26.2, and 42.9 kJ mol^{-1} for this series of dyads, in better absolute agreement with experiment.

The frontier HOMO and LUMO for the investigated dyads were obtained by the B3LYP/3-21G(*) method and are shown in Figure 5 for the representative (TPP)Zn:**5** dyad. In the studied dyads, the majority of the electron distribution of HOMO was found to be located on the (TPP)Zn entity with a small orbital coefficient on the axial pyridine or imidazole ligand, suggesting weak charge-transfer interaction between zinc porphyrin and C_{60} entities in the ground state. On the other hand, the majority of the electron distribution of LUMO was located on the C_{60} spheroid. These observations suggest the existence of charge-transfer transition from zinc porphyrin entity to the C_{60} entity. The orbital energies of the HOMO and the LUMO were found to be −4.61 and −3.57 eV for the (TPP)Zn:**4** dyad while for the (TPP)Zn:**5** dyad these values were −4.51 and −3.55 eV. The calculated HOMO−LUMO gap (gas phase) was 1.04 and 0.96 eV respectively for the (TPP)Zn:**4** and (TPP)Zn:**5** dyads.

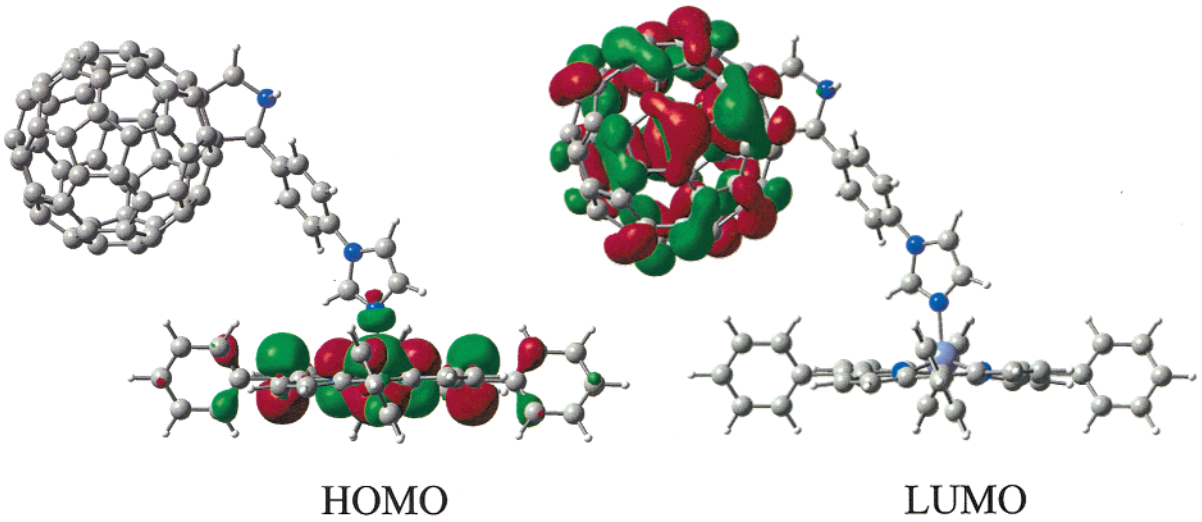

Figure 5. Ab initio B3LYP/3-21G(*) calculated frontier HOMO and LUMO for the (TPP)Zn:**5** complex.

The small HOMO−LUMO gap agreed fairly with the electrochemically measured (difference between the first oxidation and first reduction potential) values (vide infra). It may be mentioned here that only recently the validity of molecular orbitals generated by density functional methods is being recognized.[19] The accuracy of these methods, especially B3LYP, is recently being demonstrated by Schaefer and co-workers on electron affinities of aromatic compounds[20] and, more recently, on fullerene-based covalently linked dyads and triads.[10n]

Cyclic Voltammetric Studies. Determination of the redox potentials in the newly formed molecular donor−acceptor type systems is important to probe the existence of charge-transfer interactions between the donor and acceptor in the ground state, and also to evaluate the energetic of electron-transfer reactions. With this in mind, we have performed a systematic study to evaluate the redox behavior of the self-assembled dyads using cyclic voltammetric technique. The cyclic voltammogram of (TPP)Zn is shown in Figure 6c. The redox potentials corresponding to the oxidation were located at 0.28 and 0.62 V vs Fc/Fc^+ while the potentials corresponding to the reduction were located at −1.92 and −2.23 V vs Fc/Fc^+, respectively. The first three reversible reductions of **5** in 0.1 M $(TBA)ClO_4$, *o*-dichlorobenzene, were located at $E_{1/2} = -1.13$, −1.51, and −2.05 V vs Fc/Fc^+, respectively (Figure 6b). These values compare with the $E_{1/2} = -1.10$, −1.49, and −1.95 V vs Fc/Fc^+, respectively, for pristine C_{60}.[11a] Depending upon the oxidation state, a negative shift of 100 to 170 mV was observed for fulleropyrrolidine derivatives as compared to the respective redox couple of pristine C_{60}. These observations are in agreement with the earlier value reported for the other C_{60} pyrrolidine derivatives,[21] and also for the bisalkylated C_{60} derivatives.[22] Among the different fulleropyrrolidine derivatives, the redox potentials did not reveal any appreciable changes (Table 2).

The cyclic voltammogram of the self-assembled dyad (TPP)-Zn:**5**, obtained by slow precipitation, is shown in Figure 6a. Within the accessible potential window of the solvent, a total of seven reversible redox processes have been observed. The first and second redox potentials corresponding to the oxidation of the zinc porphyrin were located at $E_{1/2} = 0.29$ and 0.67 V vs Fc/Fc^+, respectively. The reduction potentials of the appended C_{60} moiety of **5** were located at $E_{1/2} = -1.10$, −1.49, and −2.02 V vs Fc/Fc^+, while the corresponding potentials for the zinc porphyrin ring reduction were located at $E_{1/2} = -1.91$ and −2.19 V vs Fc/Fc^+, respectively; that is, the reduction potentials of the C_{60} entity are positively shifted by 20−30 mV. The

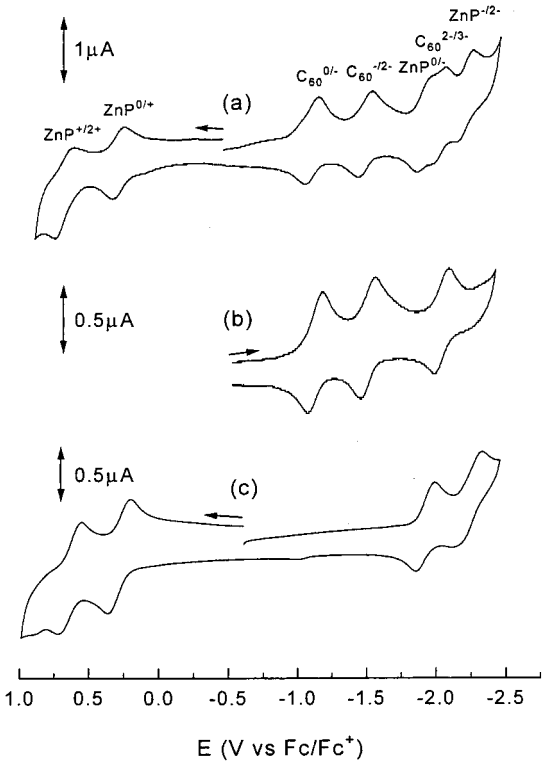

Figure 6. Cyclic voltammograms of (a) the isolated (TPP)Zn:**5** complex, (b) **5**, and (c) (TPP)Zn in *o*-dichlorobenzene, 0.1 M $(TBA)ClO_4$. Scan rate = 100 mV/s.

potential difference between the first oxidation of (TPP)Zn and the first reduction of fulleropyrrolidine in the self-assembled dyads was found to be 1.39 V, which compares fairly well with the earlier computed values. Also, the redox potentials of (TPP)Zn and C_{60} entities revealed small changes (10−20 mV) upon dyad formation (Table 2) suggesting the existence of weak charge transfer interactions, an observation that parallels the results of computational studies. However, we did not succeed in detecting a new absorption band corresponding to the charge transfer interactions in the longer wavelength region (> 610 nm). It is likely that such bands are too weak to detect. It may be mentioned here that the absorption peak at 605 nm in Figure 1 increases with increasing the concentration of **5**, mainly due to the added **5** and not due to any CT bands.

Fluorescence Quenching Experiments. The photochemical behavior of the (TPP)Zn−C_{60} dyads were investigated, first,

TABLE 2: Electrochemical Reversible Redox Potentials (vs Fc/Fc$^+$) of the Self-Assembled Zinc Tetraphenylporphyrin−Fulleropyrrolidine Conjugates in *o*-Dichlorobenzene, 0.1 M (TBA)ClO_4

	potential, V vs Fc/Fc$^+$						
compound	(TPP)Zn$^{+/2+}$	(TPP)Zn$^{0/+}$	$C_{60}^{0/-}$	$C_{60}^{-/2-}$	(TPP)Zn$^{0/-}$	$C_{60}^{2-/3-}$	(TPP)Zn$^{-/2-}$
(TPP)Zn	0.62	0.28			−1.92		−2.23
2[a]			−1.10	−1.49		−1.95	
3			−1.10	−1.50		−1.96	
5			−1.13	−1.51		−2.04	
(TPP)Zn:**2**[b]	0.64	0.29	−1.10	−1.50	−1.91	−1.96	−2.20
(TPP)Zn:**3**	0.65	0.28	−1.11	−1.50	−1.90	−1.97	−2.20
(TPP)Zn:**5**[b]	0.67	0.29	−1.10	−1.49	−1.91	−2.02	−2.19

[a] From ref 11a. [b] Obtained by slow precipitation of (TPP)Zn and **2** or **3** or **5**.

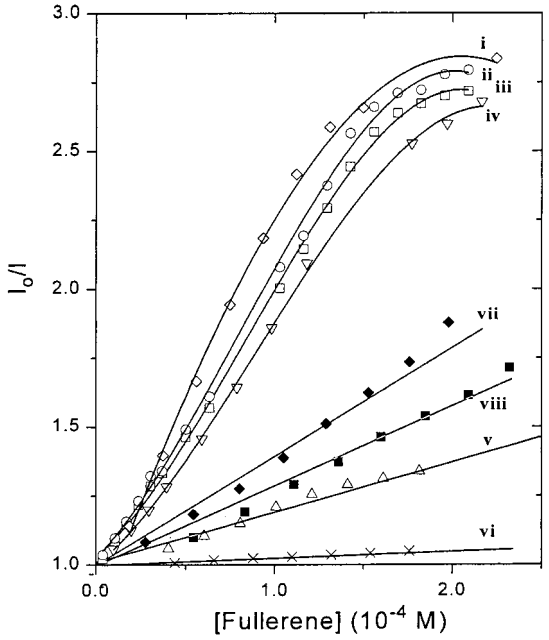

Figure 7. Stern-Volmer plots for the fluorescence quenching of (TPP)-Zn by various fulleropyrrolidines: (i) **5**, (ii) **4**, (iii) **3**, (iv) **2**, (v) **1**, and (vi) pyridine in *o*-dichlorobenzene; (vii) **5** and (viii) **3** in benzonitrile. The concentration of (TPP)Zn was 0.05 mM, $\lambda_{ex} = 554$ nm and $\lambda_{em} = 646$ nm.

by using steady-state fluorescence measurements. On addition of either of compounds **2**−**5** to a argon saturated *o*-dichlorobenzene solution of (TPP)Zn, the fluorescence intensity decreased until about 30%. Scanning the emission wavelength to longer wavelength regions (700−800 nm) revealed a weak emission band at 710 nm corresponding to the singlet emission of the C_{60} moiety. The intensity of the this band for a given concentration of fulleropyrrolidine was found to be almost the same as that obtained in the absence of added (TPP)Zn. Changing the excitation wavelength from 554 to 410 nm also revealed similar observations with slightly enhanced emission of fulleropyrrolidine due to its higher absorbance at 410 nm. Similar observations were also made in the studied benzonitrile solvent. These results suggest that the energy transfer from the singlet excited (TPP)Zn to fulleropyrrolidine is not necessarily a cause of the fluorescence quenching.

Figure 7 shows the Stern−Volmer plots for the quenching of (TPP)Zn by various fulleropyrrolidines as well as a reference compound, pyridine in *o*-dichlorobenzene (curves i−vi) and in benzonitrile (curves vii−viii). In agreement with the higher *K* values, the Stern−Volmer plots obtained for **5** revealed higher slopes followed by those for **4**-**2**. However, at higher concentrations of **2**-**5** the plots revealed a downward curvature. The bimolecular quenching constants, k_q calculated from the linear segment of the Stern−Volmer plots revealed that the k_q values are 2−3 orders of magnitude higher than that expected for diffusion controlled processes. These results suggested the occurrence of both inter- as well as intramolecular (axial coordination) photochemical events. For **1**, the amount of quenching was found to be low and the Stern−Volmer plot was found to be linear in the concentration range (plot v) while for pyridine the Stern−Volmer plot was almost parallel to the *X*-axis (plot vi). Interestingly, in benzonitrile, the quenching of (TPP)Zn fluorescence by **3** and **5** was less and the Stern−Volmer plots were linear (plots vii and viii). These results suggested that intermolecular type quenching was the main process for (TPP)Zn fluorescence quenching by **1** in *o*-dichlorobenzene; and, **3** and **5** in benzonitrile. It may be mentioned here that optical absorbance studies of binding of **3** or **5** to (TPP)Zn in benzonitrile revealed little or no spectral changes suggesting negligible amount of binding due to strong solvent coordination to the central zinc ion.

Further, the singlet emission of fulleropyrrolidine was monitored at 710 nm by exciting the samples at 380 nm where the majority of the fulleropyrrolidine was excited. It was observed that in *o*-dichlorobenzene on addition of excess of (TPP)Zn (10 equiv), the emission intensity of fulleropyrrolidine at 710 nm revealed quenching less than 10% of its original intensity (see supplementary section for spectra). Such effect was even smaller in the studied benzonitrile solvent. Excitation spectra recorded by fixing the emission monochromator at the intense 600 and 650 nm emission bands of (TPP)Zn revealed mainly the bands of (TPP)Zn. Our attempts to obtain the excitation spectrum at the weak 710 nm band of fulleropyrrolidine was not successful mainly because of the overlap of zinc porphyrin strong absorption and emission bands in the spectral region. These results suggest the absence of appreciable photochemical events occurring from the singlet excited fulleropyrrolidine to the bound (TPP)Zn.

To further understand the reaction mechanism (inter- or intramolecular) and follow the kinetics of photoinduced processes, picosecond time-resolved emission and nanosecond transient absorption studies were performed on two selected (TPP)Zn:**3** and (TPP)Zn:**5** complexes. Recently, the photochemical behavior of (TPP)Zn:**4** has been reported.[11e]

Fluorescence Lifetimes. The time-resolved fluorescence spectral features of the dyads were essentially the same as those observed by steady-state measurements. The fluorescence decay-time profile of (TPP)Zn (monitored at 600 nm) in the absence of **3** or **5** was usually fitted with a single-exponential curve (Figure 8). In the presence of excess of **3** compared with (TPP)Zn, each fluorescence decay of (TPP)Zn was accelerated only slightly, in which the decay curve was fitted with mono exponential curve in both *o*-dichlorobenzene and in benzonitrile. On addition of **5** to *o*-dichlorobenzene solution of (TPP)Zn, the fluorescence decay of (TPP)Zn was accelerated (Figure 8), in which the decay curve was fitted with two exponential curves,

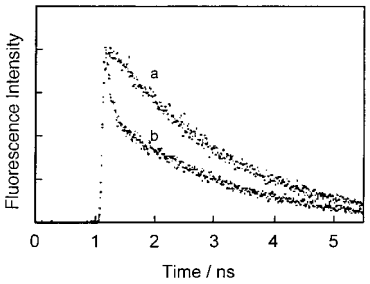

Figure 8. Fluorescence decay profiles of (TPP)Zn (0.03 mM) in (a) the absence of and (b) presence of **5** (0.2 mM) in *o*-dichlorobenzene. $\lambda_{ex} = 410$ nm, $\lambda_{cm} = 650$ nm.

TABLE 3: Fluorescence Lifetimes (τ_f), Charge-Separation Rate Constants ($k_{CS}^{singlet}$), Charge-Separation Quantum Yields ($\Phi_{CS}^{singlet}$ for Zinc Tetraphenylporphyrin−Fulleropyrrolidine Supramolecular Dyads in *o*-Dichlorobenzene (DCB) and Benzonitrile (BN) Solvents

compound	solvent	τ_f /ns (fraction %)	$k_{CS}^{singlet}/s^{-1}$	$\Phi_{CS}^{singlet}$
(TPP)Zn	DCB	2.10(100%)		
	BN	2.10(100%)		
(TPP)Zn:**3**(1:1)	DCB	1.88(100%)	5.6×10^7	0.10
	BN	1.78(100%)	8.6×10^7	0.15
(TPP)Zn:**3**(1:6)	DCB	1.85(100%)	6.3×10^7	0.12
	BN	1.78(100%)	8.6×10^7	0.15
(TPP)Zn:**5**(1:1)	DCB	0.058(30%) 2.00 (70%)	1.7×10^{10}	0.97
	BN	1.77(100%)	8.9×10^7	0.16
(TPP)Zn:**5**(1:6)	DCB	0.058 (50%) 2.00 (50%)	1.7×10^{10}	0.97
	BN	1.78(100%)	8.6×10^7	0.15

[a] $k_{CS}^{singlet} = (1/\tau_f)_{sample} - (1/\tau_f)_{ref}$. [b] $\Phi_{cs}^{singlet} = [(1/\tau_f)_{sample} - (1/\tau_f)_{ref}]/(1/\tau_f)_{sample}$.

while in benzonitrile, only slight acceleration of the fluorescence decay rate was observed. From the initial fast and the later slow decays, two fluorescence lifetimes (τ_f) were evaluated. The lifetime of the slow decay part is almost the same as that of (TPP)Zn in *o*-dichlorobenzene. Contribution of the short lifetime increased with increased addition of **5** in *o*-dichlorobenzene, indicating decreased quantities of uncomplexed (TPP)Zn.

By assuming the short lifetimes are due to the electron transfer within the supramolecular dyads, the charge-separated rates ($k_{cs}^{singlet}$) and quantum yield ($\Phi_{cs}^{singlet}$) were evaluated in a manner usually employed in the intramolecular electron-transfer process. Higher values of both $k_{cs}^{singlet}$ and $\Phi_{cs}^{singlet}$ were obtained for **5** binding to (TPP)Zn (Table 3). For **3** binding to (TPP)Zn on the other hand, both $k_{cs}^{singlet}$ and $\Phi_{cs}^{singlet}$ were found to be quite low, although the quenching of fluorescence intensity is similar to **5** (Figure 7). This suggests that the supramolecular (TPP)Zn:**3** is nonfluorescent because of close interaction between (TPP)Zn and the C_{60} moiety as shown in Figure 4a. Nonfluorescence dyad may be caused by partial charge-transfer interactions. Thus, the fluorescence of uncoordinated (TPP)Zn was observed in steady-state fluorescence spectra and lifetime measurements.

In case of supramolecular (TPP)Zn:**5**, the dyad is fluorescent although the fluorescence quantum yield is lower than uncoordinated (TPP)Zn; such difference from (TPP)Zn:**3** may be due to longer distance between (TPP)Zn and the C_{60} moiety as shown in Figure 4b, in which direct interaction between (TPP)Zn and the C_{60} moiety is unlikely.

Time-Resolved Absorption Spectra. Nanosecond transient spectra of pristine (TPP)Zn showed absorption peaks at 630 and 840 nm corresponding to its excited triplet state.[23−25] Compounds **1**−**5** showed a band at 700 nm corresponding to its excited triplet state.[24] An intriguing question in self-assembled donor−acceptor dyads is the stability of the dyads in the presence of high power laser used in transient absorption measurements. It may be pointed out here that in the present investigation both steady-state emission and fluorescence lifetime using laser light used low light power density. Hence, during fluorescence measurements, dissociation of the complexes may not be a competing process. On the other hand, high laser power with short wavelength may cause excitation to higher excited states or higher vibronic levels, which would enhance the chance of complex dissociation. In the present study, we have employed nanosecond laser light with longer wavelength ($\lambda = 530$ nm) to avoid such dissociation of the complex before charge separation. As discussed later in this section, the observed quick rise and decay at 1000 nm corresponding to C_{60} anion radical, is strong evidence for the charge separation prior to any dissociation.

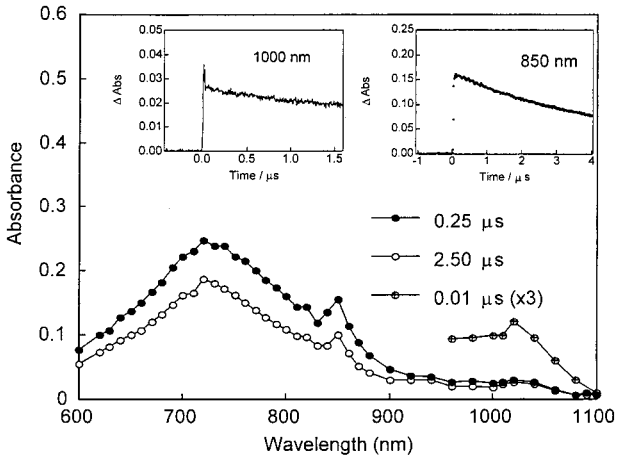

Figure 9. Transient absorption spectra obtained using 530 nm laser excitation for (TPP)Zn (0.05 mM) in the presence of **5** (0.5 mM) [ratio = 1:6] in Ar-saturated *o*-dichlorobenzene. Inset: Time profiles for the 850 and 1000 nm bands.

On addition of excess of **5** to (TPP)Zn (6:1 equiv) in *o*-dichlorobenzene, an intense band at 700 nm corresponding to the triplet state of **5** was observed. A weak peak at 1000 nm also appeared at a time interval of 0.01 μs (Figure 9); this was assigned to the radical anion of the C_{60} moiety. The time profile at 1000 nm in the inset figure shows the observed quick rise-decay, which indicates the supramolecular ion-pair formation via the singlet state of (TPP)Zn. The charge recombination rate of the supramolecular ion-pair was as fast as nanosecond laser pulse and time-resolution of the detector (about 10 ns); $<10^8$ s^{-1}. The intermolecular rate constants for electron transfer from ^{3}(TPP)Zn* to the ground state **5** (k_{et}^T) was not prominent in *o*-dichlorobenzene, because the slow rise was not observed at 1000 nm.

In benzonitrile, however, the transient absorption spectra showed quite different features. In the presence of excess **5** to (TPP)Zn (6:1 equiv), the triplet absorption bands at 840 and 700 nm decayed faster than those in *o*-dichlorobenzene. Furthermore, a slow rise was clearly observed at the 1020 nm band of the anion radical of **5** in addition to the quick rise-decay. Corresponding to the slow rise of the anion radical of **5**, the rise of the radical cation of (TPP)Zn was also observed at 600 nm, although this band overlapped with other species in this wavelength region. These observations suggest that intermolecular electron transfer via the triplet state of (TPP)Zn is predominant in benzonitrile. The k_{et}^T value was evaluated to be ca. ca. 5×10^7 M^{-1} s^{-1}, on the basis of $\Phi_{et}^T = 1.0$. In

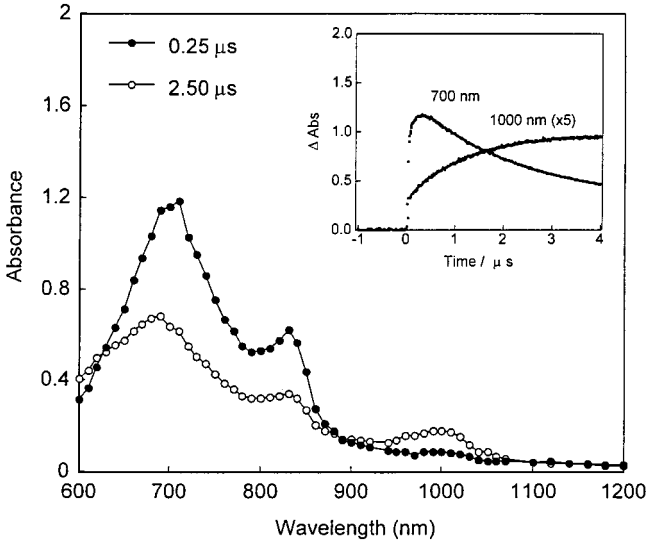

Figure 10. Transient absorption spectra obtained by the 530 nm nanosecond laser photolysis of (TPP)Zn−**3** (0.05 mM:0.3 mM) in benzonitrile. Inset: Time profiles for the 700 and 1000 nm bands.

benzonitrile, however, the Φ_{et}^{T} value is usually about 0.5; thus the estimated k_{et}^{T} value is about 2.5×10^7 M^{-1} s^{-1}. For the quantum yield calculations, the molar absorption coefficients for the fulleropyrrolidine anion radicals and fulleropyrrolidine triplet states were assumed to be 8.85×10^3 [26] and 1.4×10^4 M^{-1} cm^{-1},[27] respectively.

In case of **3**, similar transient spectra were observed in *o*-dichlorobenzene but in benzonitrile, the transient absorption spectrum obtained for (TPP)Zn:**3** (1:6 eq) revealed an increase of the C_{60} radical anion band with the decay of the triplet states of the components (Figure 10). This observation is quite different from the quick rise-decay of the radical anion of C_{60} moiety in *o*-dichlorobenzene. The presence of oxygen in solution is found to promote the decay of the triplet state of **3**. The initial sharp part of the quick rise-decay time profile of the radical anion of **3** in *o*-dichlorobenzene was not affected by oxygen, but the slow decay part was almost completely quenched, indicating the slow part is the absorption tail of the triplet states. However, the calculated low values of $k_{CS}^{singlet}$ and $\Phi_{cs}^{singlet}$ from the fluorescence lifetime measurements suggests that the nonfluorescent (TPP)Zn:**3** dyad is charge-separated by the direct laser excitation of the dyads without passing through the excited singlet state of (TPP)Zn. Such intramolecular electron transfer may be possible by the close distance between (TPP)Zn and the C_{60} moiety (Figure 4).

Importantly, in benzonitrile, the evaluated k_{et}^{T} value for the (TPP)Zn:**3** dyad was found to be ca. 5×10^8 M^{-1} s^{-1}, which is 20 times greater than that of (TPP)Zn:**5**. Since the reduction potentials of **3** and **5** are almost the same, the steric effects caused by the long pendant phenyl imidazole group might be responsible for this observation. An attempt was also made here to analyze decay kinetics of the ion pairs in benzonitrile from the back electron-transfer rate, k_{bet} constants. The decays of the anion radicals of the C_{60} were monitored in the long time scale-up to several hundred microseconds. The decays followed a second-order reaction kinetics indicating that the back electron transfer takes place in a bimolecular reaction pathway involving the solvated anion and cation radicals. The slope of the second-order reaction plot ($1/\Delta$abs vs time) yielded the ratio of k_{bet} to the molar absorption coefficients of the fulleropyrrolidine anion radical. The k_{bet} values calculated from this approach for (TPP)Zn:**3** and (TPP)Zn:**5** dyads in benzonitrile were found to

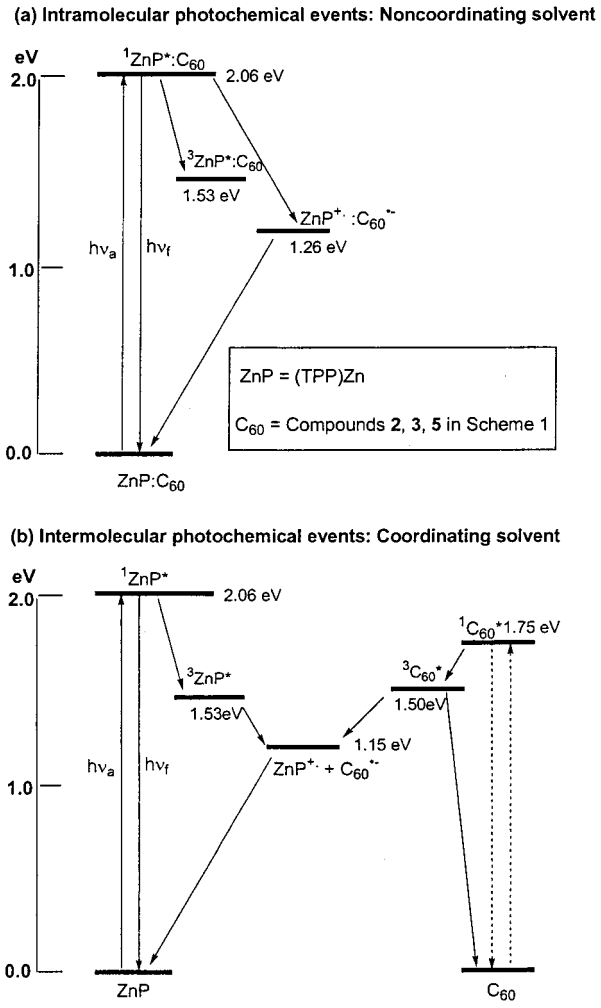

Figure 11. Energy level diagrams showing the different photochemical events of (a) intramolecular and (b) intermolecular (TPP)Zn interacting with fulleropyrrolidine dyads.

be 8.6×10^9 and 8.4×10^9 M^{-1} s^{-1}, respectively, which are close to the diffusion controlled limit. Since the concentrations of the cation and anion radicals are quite lower than the reactants, the observed decay rates of the backward process are far slower than that of the forward process, even though $k_{bet} \gg k_{et}$.

Summary

We have demonstrated the formation of porphyrin−fullerene supramolecular dyads by axial coordination of fulleropyrrolidine bearing either pyridine or imidazole ligands with (TPP)Zn. The UV−vis, ^{1}H NMR, and ESI-mass spectral studies revealed 1:1 molecular stoichiometry between the donor, (TPP)Zn and the acceptor, fulleropyrrolidine entities. The determined formation constants *K* follow the order *o*-pyridyl ≪ *m*-pyridyl ≃ *p*-pyridyl ≪ *N*-phenyl imidazole entities of the fulleropyrrolidine: that is, they are controlled by the nature of the axial ligand and the associated steric factors. The geometric and electronic structure of the dyads probed using ab initio B3LYP/3-21G(*) methods revealed stable complexation between the donor, (TPP)Zn and the acceptor, fulleropyrrolidine entities. Cyclic voltammetric studies revealed a total of seven one-electron redox processes within the accessible potential window of *o*-dichlorobenzene, 0.1 (TBA)ClO_4. The experimentally calculated HOMO−LUMO gap for the studied dyads compared fairly well with the computed one. As summarized in energy level diagram of Figure

11, the results of the steady-state and time-resolved emission, and transient absorption studies revealed the occurrence of electron transfer mainly from the singlet excited zinc porphyrin to the fullerene entity in the noncoordinating solvent, *o*-dichlorobenzene. However, the main quenching pathway in the coordinating solvent, benzonitrile is shown to take place via an intermolecular electron-transfer from the triplet excited (TPP)Zn to the C_{60} entity. The present studies also revealed little or no photochemical events occurring from the singlet excited fulleropyrrolidine to the (TPP)Zn in the bound or the unbound forms.

Acknowledgment. The authors are thankful to the donors of the Petroleum Research Fund, administered by the American Chemical Society, National Science Foundation (CCLI and A&I), National Institutes of Health (to F.D.), and to the Dreyfus Foundation (to M.E.Z.) for support of this work. The authors are also thankful to the High Performance Computing Center of the Wichita State University for lending SGI ORIGIN 2000 computer time. Vu T. Hoang is thankful to the McNair Scholars Program for an undergraduate minority student scholarship.

Supporting Information Available: ESI-mass of (TPP)Zn:**3** dyad in CH_2Cl_2; B3LPY/3-21G(*) calculated frontier HOMO and LUMO for the (TPP)Zn:**4** dyad; steady-state emission spectra of (TPP)Zn on increasing addition of **5**, and for **3** in the presence and absence of (TPP)Zn; transient absorption spectra of (TPP)Zn:**3** (1:1) in *o*-dichlorobenzene, (TPP)Zn:**3** (1:6) in *o*-dichlorobenzene, and (TPP)Zn:**3** (1:6) in o-dichlorobenzene; and time profiles at 700 and 1000 nm for the transients of (TPP)Zn:**3** (1:6) in the presence and absence of oxygen. This material is available free of charge via the Internet at http://pubs.acs.org.

References and Notes

(1) (a) Maruyama, K.; Osuka, A. *Pure Appl. Chem*. **1990**, *62*, 1511. (b) Gust, D.; Moore, T. A. *Science* **1989**, *244*, 35. (c) Gust, D.; Moore, T. A. *Top. Curr. Chem*. **1991**, *159*, 103. (d) Gust, D.; Moore, T. A.; Moore, A. L. *Acc. Chem. Res*. **1993**, *26*, 198. (e) Wasielewski, M. R. *Chem. Rev*. **1992**, *92*, 435. (f) Paddon-Row, M. N. *Acc. Chem. Res*. **1994**, *27*, 18. (g) Sutin, N. *Acc. Chem. Res*. **1983**, *15*, 275. (h) Bard, A. J.; Fox, M. A. *Acc. Chem. Res*. **1995**, *28*, 141. (i) Meyer, T. J. *Acc. Chem. Res.* **1989**, *22*, 163. (j) Piotrowiak, P. *Chem. Soc. Rev*. **1999**, *28*, 143.

(2) (a) Ward, M. W. *Chem. Soc. Rev*. **1997**, *26*, 365 and references therein. (b) Hayashi, T.; Ogoshi, H. *Chem. Soc. Rev*. **1997**, *26*, 355. (c) Sessler, J. S.; Wang, B.; Springs, S. L.; Brown, C. T. In *Comprehensive Supramolecular Chemistry*; Atwood, J. L., Davies, J. E. D., MacNicol, D. D.,Vögtle, F., Eds.; Pergamon: Elmsford, NY, 1996; Chapter 9. (d) Feldheim D. L.; Keating, C. D. *Chem. Soc. Rev*. **1998**, *27*, 1. (e) *Introduction of Molecular Electronics*; Petty, M. C., Bryce, M. R., Bloor, D., Eds.; Oxford University Press: New York, 1995. (f) Emmelius, M.; Pawlowski, G.; Vollmann, H. W *Angew. Chem., Int. Ed. Engl*. **1989**, *28*, 1445.

(3) (a) Kroto, H. W.; Heath, J. R.; O'Brien, S. C.; Curl R. F.; Smalley, R. E. *Nature* **1985**, *318*, 162. (b) Kratschmer, W.; Lamb, L. D.; Fostiropoulos F.; Huffman, D. R. *Nature* **1990**, *347*, 345.

(4) Guldi, D. M. *Chem. Commun*. **2000**, 321.

(5) Hirsch, A., Ed. *Fullerene and Related Structures*; Springer: Berlin, 1999; Vol. 199.

(6) (a) Allemand, P. M.; Koch, A.; Wudl, F.; Rubin, Y.; Diederich, F.; Alvarez, M. M.; Anz S. J.; Whetten, R. L. *J. Am. Chem. Soc*. **1991**, *113*, 1050. (b) Xie, Q.; Perez-Cordero, E.; Echegoyen, L. *J. Am. Chem. Soc*. **1992**, *114*, 3978.

(7) Ajie, H.; Alvarez, M. M.; Anz, S. J.; Beck, R. E.; Diederich, F.; Fostiropoulos, K.; Huffman, D. R.; Kratschmer, W.; Rubin, Y.; Schriver, K. E.; Sensharma E.; Whetten, R. L. *J. Phys. Chem*. **1990**, *94*, 8630.

(8) (a) Khan, S. I.; Oliver, A. M.; Paddon-Row, M. N.; Rubin, Y. *J. Am. Chem. Soc*. **1993**, *115*, 4919. (b) Saricciftci, N. S.; Wudl, F.; Heeger, A. J.; Maggini, M.; Scorrano, G.; Prato, M.; Bourassa, J.; Ford, P. C. *Chem. Phys. Lett*. **1995**, *247*, 510. (c) Liddell, P. A.; Sumia, J. P.; Macpherson, A. N.; Noss, L.; Seely, G. R.; Clark, K. N.; Moore, A. L.; Moore T. A.; Gust, D. *Photochem. Photobiol*. **1994**, *60*, 537. (d) Williams, R. M.; Zwier, J. M.; Verhoever, J. W. *J. Am. Chem. Soc*. **1995**, *117*, 4093. (e) Imahori, H.; Hagiwara, K.; Aoki, M.; Akiyama, T.; Taniguchi, S.; Okada, T.; Shirakawa, M.; Sakata, Y. *J. Am. Chem. Soc*. **1996**, *118*, 11771. (f) Kuciauskas, D.; Lin, S.; Seely, G. R.; Moore, A. L.; Moore, T. A.; Gust, D.; Drovetskaya, T.; Reed, C. A.; Boyd, P. D. W. *J. Phys. Chem*. **1996**, *100*, 15926. (g) Guldi, D. M.; Maggini, M.; Scorrano, G.; Prato. M. *J. Am. Chem. Soc.* **1997**, *119*, 974. (h) Imahori, H.; Yamada, K.; Hasegawa, M.; Taniguchi, S.; Okada, T.; Sakata, Y. *Angew. Chem., Int. Ed. Engl*. **1997**, *36*, 2626. (h) Liddell, P. A.; Kuciauska, D.; Sumida, J. P.; Nash, B.; Nguyen, D.; Moore, A. L.; Moore, T. A.; Gust, D. *J. Am. Chem. Soc*. **1997**, *119*, 1400.

(9) (a) Dietel, E.; Hirsh, A.; Eichhorn, E.; Rieker, A.; Hackbarth, S.; Roder, B. *Chem. Commun*. **1998**, 1981. (b) Gareis, T.; Kothe, O.; Daub, J. *Eur. J. Org. Chem*. **1998**, 1549. (c) Da Ros, T.; Prato, M.; Guldi, D.; Alessio, E.; Ruzzi, M.; Pasimeni, L.; Carano, M.; Paolucci, F.; Ceroni, P.; Roffia, S. In *Recent Advances in the Chemistry and Physics of Fullerenes and Related Materials*; Kadish, K. M., Ruoff, R. S., Eds.; The Electrochemical Proceedings Series; The Electrochemical Society: Pennington, NJ, 1998; p 1074. (d) Martin, N.; Sanchez, L.; Illescas, B.; Perez, I. *Chem. Rev*. **1998**, *98*, 2527. (e) Gareis, T.; Kothe, O.; Daub, J. *Eur. J. Org. Chem*. **1998**, 1549.

(10) (a) Imahori, H.; Tamaki, K.; Guldi, D. M.; Luo, C.; Fujitsuka, M.; Ito, O.; Sakata, Y.; Fukuzumi, S. *J. Am. Chem. Soc.* **2001**, *123*, 2607. (b) Armaroli, N.; Marconi, G.; Echegoyen, L.; Bourgeois, J.-P.; Diederich, F. *Chem. Eur. J*. **2000**, *6*, 1629. (c) Guildi, D. M.; Luo, C.; Da Ros, T.; Prato, M.; Dietel, E.; Hirsch, A. *Chem. Commun*. **2000**, 375. (d) Luo, C.; Guldi, D. M.; Imahori, H.; Tamaki, K.; Sakata, Y. *J. Am. Chem. Soc*. **2000**, *122*, 6535. (e) Kuciauskas, D.; Liddell, P. A.; Lin, S.; Stone, S. G.; Moore, A. L.; Moore, T. A.; Gust, D. *J. Phys. Chem. B* **2000**, *104*, 4307. (f) Schuster, D. I.; Cheng, P.; Wilson, S. R.; Prokhorenko, V.; Katterie, M.; Holzwarth, A. R.; Braslavsky, S. E.; Klihm, G.; Williams, R. M. Luo, C. *J. Am. Chem. Soc*. **2000**, *121*, 11599. (g) Tashiro, K.; Aida, T.; Zheng, J.-Y.; Kinbara, K.; Saigo, K.; Sakamoto, S.; Yamaguchi, K. *J. Am. Chem. Soc*. **1999**, *121*, 9477. (h) Tkachenko, N. V.; Rantala, L.; Tauber, A. Y.; Helaja, J.; Hynninen, P. H.; Lemmetyinen, H. *J. Am. Chem. Soc*. **1999**, *121*, 9378. (i) Imahori, H.; Norieda, H.; Yamada, H.; Nishimura, Y.; Yamazaki, I.; Sakata, Y.; Fukuzumi, S. *J. Am. Chem. Soc.* **2001**, *123*, 100. (j) Imahori, H.; Tkachenko, N. V.; Vehmanen, V.; Tamaki, K.; Lemetyinen, H.; Sakata, T.; Fukuzumi, S. *J. Phys. Chem. A* **2001**, *105*, 1750. (k) Fukuzumi, S.; Imahori, H.; Yamada, H.; El-Khouly, M. E.; Fujitsuka, M.; Ito, O.; Guldi, D. M. *J. Am. Chem. Soc*. **2001**, *123*, 2571. (l) Imahori, H.; Tamaki, K.; Guldi, D. M.; Luo, C.; Fujitsika, M.; Ito, O.; Sakata, Y.; Fukuzumi, S. *J. Am. Chem. Soc*. **2001**, *123*, 2607. (m) Imahori, H.; Guldi, D. M.; Tamaki, K.; Yoshida, Y.; Luo, C.; Sakata, Y.; Fukuzuzmi, S. *J. Am. Chem. Soc*. **2001**, *123*, 6617. (n) D'Souza, F.; Zandler, M. E.; Smith, P. M.; Deviprasad, G. R.; Klykov, A.; Fujitsuka, M.; Ito, O. *J. Phys. Chem. A* **2002**, *106*, 649.

(11) (a) D'Souza, F.; Deviprasad, G. R.; Rahman, M. S.; Choi, J.-P. *Inorg. Chem*. **1999**, *38*, 2157. (b) Armaroli, N.; Diederich, F.; Echegoyen, L.; Habicher, T.; Flamigni, L.; Marconi, G.; Nierengarten,. J.-F. *New. J. Chem*. **1999**, 77. (c) Da Ros, T.; Prato, M.; Guldi, D. M.; Alessio, E.; Ruzzi, M.; Pasimeni, L. *Chem. Commun*. **1999**, 635. (d) D'Souza, F.; Rath, N. P.; Deviprasad, G. R.; Zandler, M. E. *Chem. Commun*. **2001**, 267. (e) Da Ros, T.; Prato, M.; Guldi, D. M.; Ruzzi, M.; Pasimeni, L. *Chem. Eur. J*. **2001**, *7*, 816. (f) D'Souza, F.; Deviprasad, G. R.; El-Khouly, M. E.; Fujitsuka, M.; Ito, O. *J. Am. Chem. Soc*. **2001**, *123*, 5277.

(12) D'Souza, F.; Zandler, M. E.; Deviprasad, G. R.; Kutner, W. *J. Phys. Chem. A* **2000**, *104*, 6887.

(13) Smith, K. M. *Porphyrins and Metalloporphyrins*; Elsevier: New York, 1977.

(14) Maggini, M.; Scorrano, G.; Prato, M. *J. Am. Chem. Soc*. **1993**, *115*, 9798.

(15) Frisch, M. J.; Trucks, G. W.; Schlegel, H. B.; Scuseria, G. E.; Robb, M. A.; Cheeseman, J. R.; Zakrzewski, V. G.; Montgomery, J. A.; Stratmann, R. E.; Burant, J. C.; Dapprich, S.; Millam, J. M.; Daniels, A. D.; Kudin, K. N.; Strain, M. C.; Farkas, O.; Tomasi, J.; Barone, V.; Cossi, M.; Cammi, R.; Mennucci, B.; Pomelli, C.; Adamo, C.; Clifford, S.; Ochterski, J.; Petersson, G. A.; Ayala, P. Y.; Cui, Q.; Morokuma, K.; Malick, D. K.; Rabuck, A. D.; Raghavachari, K.; Foresman, J. B.; Cioslowski, J.; Ortiz, J. V.; Stefanov, B. B.; Liu, G.; Liashenko, A.; Piskorz, P.; Komaromi, I.; Gomperts, R.; Martin, R. L.; Fox, D. J.; Keith, T.; Al-Laham, M. A.; Peng, C. Y.; Nanayakkara, A.; Gonzalez, C.; Challacombe, M.; Gill, P. M. W.; Johnson, B. G.; Chen, W.; Wong, M. W.; Andres, J. L.; Head-Gordon, M.; Replogle, E. S.; Pople, J. A. *Gaussian 98* (Revision A.7); Gaussian, Inc.: Pittsburgh, PA, 1998.

(16) (a) Matsumoto, K.; Fujitsuka, M.; Sato, T.; Onodera, S.; Ito, O. *J. Phys. Chem. B* **2000**, *104*, 11632. (b) Komamine, S.; Fujitsuka, M.; Ito, O.; Morikawa, K.; Miyata, T.; Ohno, T. *J. Phys. Chem. A* **2000**, *104*, 11497.

(17) (a) D'Souza, F.; Hsieh, Y.-Y.; Deviprasad, G. R. *Inorg. Chem*. **1996**, *35*, 5747. (b) Nappa, M.; Valentine, J. S. *J. Am. Chem. Soc*. **1978**, *100*, 5075.

(18) Scatchard, G. *Ann. N. Y. Acad. Sci*. **1949**, *51*, 661.

(19) Stowasser, R.; Hoffmann, R. *J. Am. Chem. Soc*. **1999**, *121*, 3414.

(20) (a) Brown, S. T.; Rienstra-Kiracofe, J. C.; Schaefer, H. F. *J. Phys. Chem. A* **1999**, *103*, 4065. (b) Rienstra-Kiracofe, J. C.; Barden, C. J.; Brown, S. T.; Schaefer, H. F. *J. Phys. Chem. A* **2001**, *105*, 524.

(21) (a) Prato, M.; Maggini, M.; Giacometti, C.; Scorrano, G.; Sandona, G.; Farnia, G. *Tetrahedron* **1996**, *52*, 5221. (b) Kutner, W.; Noworyta, K.; Deviprasad, G. R.; D'Souza, F. *J. Electrochem. Soc*. **2000**, *147*, 2647.

(22) (a) Caron, C.; Subramanian, R.; D'Souza, F.; Kim, J.; Kutner, W.; Jones, M. T.; Kadish, K. M. *J. Am. Chem. Soc*. **1993**, *115*, 8505. (b) D'Souza, F.; Caron, C.; Subramanian, R.; Kutner, W.; Jones, M. T.; Kadish, K. M. In *Recent Advances in the Chemistry and Physics of Fullerenes and Related Materials*; Kadish, K. M., Ruoff, R. S., Eds.; The Electrochemical Society Proceedings Series; The Electrochemical Society: Pennington, NJ, 1994; p 768.

(23) Imahori, H.; El-Khouly, M. E.; Fujitsuka, M.; Ito, O.; Sakata, Y.; Fukuzumi, S. *J. Phys. Chem. A* **2001**, *105*, 325.

(24) Nojiri, T.; Watanabe, A.; Ito, O. *J. Phys. Chem. A* **1998**, *102*, 5215.

(25) (a) Ghosh, H. N.; Pal, H.; Sapre, A. V.; Mittal J. P. *J. Am. Chem. Soc*. **1993**, *115*, 11722. (b) Fujitsuka, M.; Ito, O.; Yamashiro, T.; Aso, Y.; Otsubo, T. *J. Phys. Chem. A* **2000**, *104*, 4876.

(26) Luo, C.; Fujitsuka, M.; Huang, C.-H.; Ito, O. *Phys. Chem. Chem. Phys.* **1999**, *1*, 2923.

(27) Luo, C.: Fujitsuka, M.; Watanabe, A.; Ito, O.; Gan, L.; Hung, Y.; Hung, C.-H. *J. Chem. Soc., Faraday Trans.* **1998**, *94*, 527.